GLASS ELECTRON MICROPROBE ANALYSIS METHODS, PRECISION AND ACCURACY FOR TEPHRA STUDIES IN ALASKA

Matthew W. Loewen, Kristi Wallace, Jordan Lubbers, Cheryl Cameron, Dawn Ruth, Pavel Izbekov, Jessica Larsen, and Nathan Graham

Miscellaneous Publication 174

2023
STATE OF ALASKA
DEPARTMENT OF NATURAL RESOURCES
DIVISION OF GEOLOGICAL & GEOPHYSICAL SURVEYS

STATE OF ALASKA
Mike Dunleavy, Governor

DEPARTMENT OF NATURAL RESOURCES
John Boyle, Commissioner

DIVISION OF GEOLOGICAL & GEOPHYSICAL SURVEYS
Kenneth Papp, Acting State Geologist & Director

Publications produced by the Division of Geological & Geophysical Surveys are available to download from the DGGS website (dggs.alaska.gov). Publications on hard-copy or digital media can be examined or purchased in the Fairbanks office:

Alaska Division of Geological & Geophysical Surveys (DGGS)
3354 College Road | Fairbanks, Alaska 99709-3707
Phone: 907.451.5010 | Fax 907.451.5050
dggspubs@alaska.gov | dggs.alaska.gov

DGGS publications are also available at:

Alaska State Library, Historical
Collections & Talking Book Center
395 Whittier Street
Juneau, Alaska 99801

Alaska Resource Library and
Information Services (ARLIS)
3150 C Street, Suite 100
Anchorage, Alaska 99503

Suggested citation:
Loewen, M.W., Wallace, K.L., Lubbers, Jordan, Ruth, Dawn, Izbekov, P.E., Larsen, J.F., and Graham, Nathan, 2023, Glass electron microprobe analyses methods, precision and accuracy for tephra studies in Alaska: Alaska Division of Geological & Geophysical Surveys Miscellaneous Publication 174, 22 p.
https://doi.org/10.14509/31045

GLASS ELECTRON MICROPROBE ANALYSIS METHODS, PRECISION AND ACCURACY FOR TEPHRA STUDIES IN ALASKA

Matthew W. Loewen[1], Kristi Wallace[1], Jordan Lubbers[1], Dawn Ruth[2], Pavel Izbekov[3], Jessica Larsen[4], and Nathan Graham[4]

ABSTRACT

This publication reports analytical conditions and secondary standard results for electron probe microanalysis (EPMA) of glass in support of tephra studies in Alaska between 2018 and 2023. Long-term accuracy and precision are evaluated for our standardized method and compared between analytical sessions and instruments at the University of Alaska Fairbanks (UAF) and the U.S. Geological Survey (USGS) Menlo Park, California. Future versions will provide updates with secondary standard results from future analytical sessions and any changes to the analytical routine and conditions.

INTRODUCTION

This report and accompanying data files detail methods, list individual secondary standard analyses, and summarize the accuracy and precision of volcanic glass EPMA data for analyzing Alaska tephra matrix glass samples. This report covers analyses made between 2018 and 2023, during which an effort was made to standardize the analytical setup, although slight variations in calibration and processing did occur. The goal of this standard routine, and in comparing multi-year secondary standard results, is to ensure that data for unknown sample analyses is precise and comparable. This standard will enable us to correlate tephra units better and detect changes in composition at a volcano over time. Digital data accompanying this report can be downloaded from doi.org/10.14509/31045.

This approach follows the global tephra community best practice guidelines endorsed by the IAVCEI Commission on Tephrochronology (formally INTAV; Kuehn and others, 2011; Wallace and others, 2022). By aggregating multi-year secondary standard data, we provide a transparent and complete estimate of result accuracy and precision for projects that collect data over multiple years and for comparison between different projects using the same method.

We prepared a traveling mount of secondary standards that can be used on multiple instruments in different laboratories (fig. 1) because microbeam standards or reference materials often suffer heterogeneities at small scales and between individual aliquots (chips of materials or single crystals; Jarosewich and others, 1980). Thus, we can ensure our standard analyses

[1] U.S. Geological Survey, Alaska Volcano Observatory, 4210 University Dr, Anchorage, AK 99508
[2] U.S. Geological Survey, Volcano Science Center, 345 Middlefield Rd, Menlo Park, CA 94025
[3] University of Alaska Fairbanks, Department of Geosciences, P.O. Box 755790, Fairbanks, AK 99775

are directly comparable and independently verify compositions of internal lab standards. This mount includes five natural volcanic glasses: two low-silica glasses (VG-2, A-99) and three high-silica glasses (VG-568, RLS-132, KN-18). Three of these standards (VG-2, A-99, VG-568) were provided by the Smithsonian Museum of Natural History and are readily available to the analytical community[4].

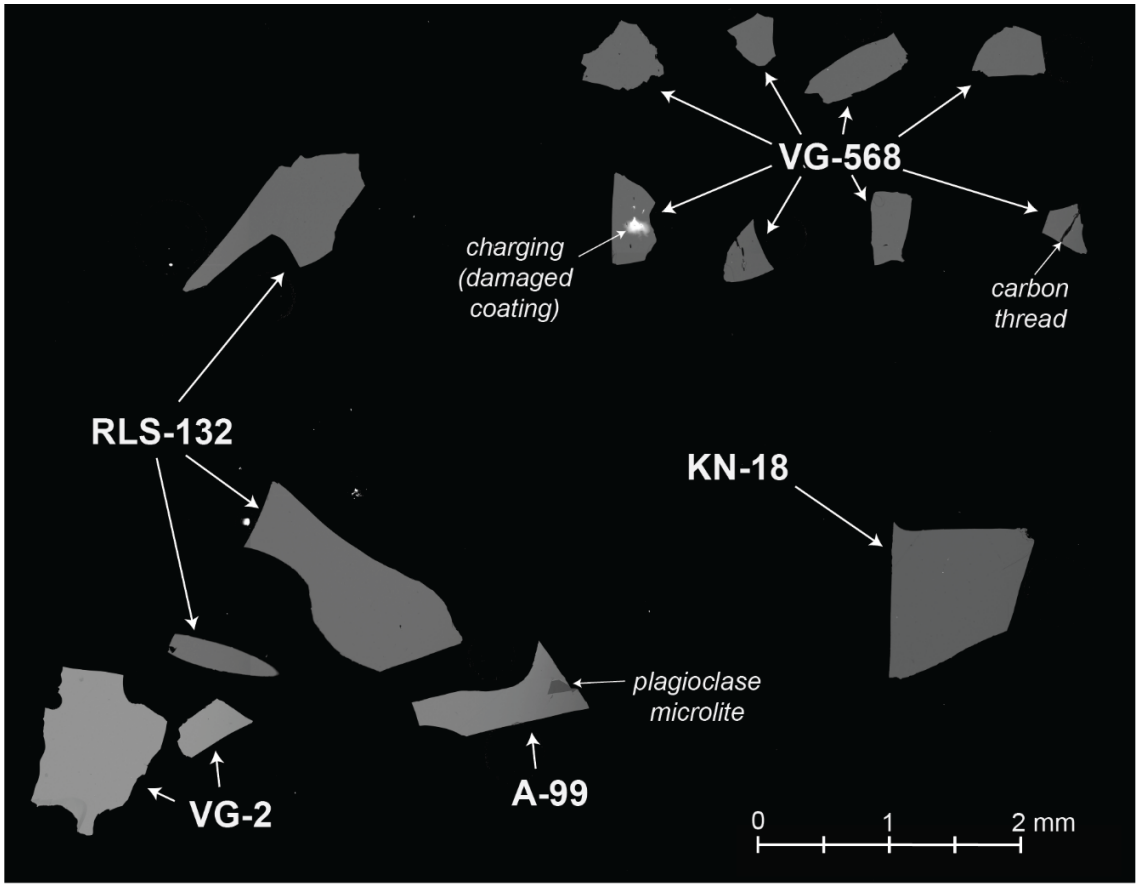

Figure 1. Backscatter electron image and chip identification of secondary standards on the traveling mount used in this study.

METHODS

We mounted unknown tephra samples with epoxy in 25-mm-diameter rounds (hereafter called "round mounts") or on commercially produced polished petrographic sections. We progressively polished round mounts with diamond grit to 1 µm and a final polish with 0.05 µm colloidal silica or 0.1 µm alumina suspension. Petrographic section preparation followed vendor protocols but typically included a final polish of 0.1 µm or finer. Our traveling standard mount was in a 25 mm-diameter round mount. Samples and calibration standards were all carbon-coated to ~22 nm thickness (indigo-blue interference on brass monitors).

[4] naturalhistory.si.edu/research/mineral-sciences/collections-overview/reference-materials/smithsonian-microbeam-standards

Analyses were performed at the UAF Advanced Instrumentation Laboratory and the USGS Electron Microprobe in Menlo Park, California.

UAF analyses reported here used a JEOL JXA 8530F electron microprobe. Tephra matrix analyses were performed at 15 kV, 10 nA, and a 5 μm defocused beam. Identical beam conditions were used on the Menlo Park JEOL JXA 8530F+ electron microprobe. Calibration standards, spectrometer assignments, peak and background count times, and time-dependent intensity corrections are summarized for each analyte in **Conditions** and **Calibrants** data tables, and attempts were made to keep these values constant over all sessions. However, some variations occurred and are noted. All elements were measured on Kα lines with linear background corrections. Data were collected and processed with Probe for EPMA software (Probe Software 2023). In UAF analyses, Na, K, and Al were measured first and corrected with a time-dependent intensity correction (TDI; Nielsen and Sigurdsson, 1981). Menlo Park analyses did not implement a TDI correction for the analyses reported here. All cations were obtained from raw intensities using the Phi-Rho-Z intensity corrections (Armstrong, 1988), while oxygen was calculated by cation stoichiometry; however, oxygen equivalent for halogens (Cl) was not used.

ACCURACY AND PRECISION

Multiple secondary standard basalts and rhyolite glasses were run throughout all analytical sessions, and individual secondary standard point analyses are provided in the **SecondaryStandardResults** data file. We consider precision after normalization to 100 percent anhydrous (but including Cl), with Fe concentrations calculated as the total Fe (denoted by FeOT) and compared to normalized "accepted" values (**SecondaryStandardValues** data table) to determine accuracy. Normalization corrects many anomalously low or high totals (above or below a 100 percent total), which, through our examination, appear to affect all elements proportionally. Normalization is often necessary for analyzing unknown tephra that may be affected by secondary hydration resulting in low totals, or where analysis of thin glass on bubble walls results in low totals. Although this is less of an issue for the secondary standards presented here, we prefer to treat our secondary standards similarly to our unknowns to provide the most accurate representation of unknown analysis accuracy and precision.

Our traveling secondary standard mount was incorporated into analyses as an unknown block one or more times per analytical session. It included Smithsonian standard glasses VG-2 (NMNH 111240-52), A-99 (NMNH 113498-1), VG-568 (NMNH 72854), USGS standard RLS-132, and KN-18. Four of the measured standards were part of the UAF EPMA internal standard block and had unique names BG-1 ("VG-2_UAF"), BG-2 ("A-99_UAF"), BG-3 (NMNH 113716-1), Rhyolite ("VG-568_UAF"), and CCNM (also known as "Lipari" UA5831). An internal aliquot of VG-2 was also analyzed on the USGS Menlo Park microprobe ("VG-2_cal") along with an internal rhyolite (RLS-75). Accepted values for Smithsonian glasses are from Jarosewich and others (1980), except for Mg on VG-2 from Helz and others (2014), and Cl concentrations from various sources compiled on the Smithsonian NMNH website[5] RLS-132 values are reported in Macdonald and others (1992). All our accepted values and their referenced sources are provided in the **SecondaryStandardValues** data table.

We report summary reproducibility as 2σ relative percentages for all secondary standards in table 1 for the aggregated analyses of secondary standards in all analytical sessions and in both labs. Relative 2σ reproducibility for SiO_2 is 0.5 to 1.5 percent for all standards (n = 20–184). Other oxide

uncertainties are strongly correlated with concentration, where expected uncertainties are exponentially higher at lower concentrations (fig. 2): <5 percent uncertainties are typical for major oxides >5 wt.% concentration and ~5–10 percent uncertainties for 1–5 wt.% concentrations. Minor oxides (0.1–1 wt.%) have 10–20 percent uncertainties, and trace element (<0.1 wt.%) uncertainties were generally poor (approaching 100 percent as concentration nears detection limit). Na_2O reproducibility was notably worse, specifically for UAF EPMA internal standards BG-3, VG-568_UAF, and CCNM. We suspect this is due to cumulative Na migration and beam damage to these heavily used internal standard aliquots. In a SiO_2–Na_2O diagram, Na depletion correlates with increased Si, a common trend observed with Na migration (fig. 3). We do not see the same trend in our external working standard mount of VG-568, which is the same material analyzed in the same session, suggesting this trend is due to the material differences and not those in analytical conditions or processing. In fact, the stability of Na on our VG-568 mount suggests that the combined defocused 5 µm beam, 10 nA current, and TDI correction compensate well for any Na loss.

Table 1. The precision of repeat secondary standard analysis reported as 2σ relative %. Concentrations approximating zero return undefined "infinite" relative precisions and are displayed as "Inf."

Standard	SiO_2	TiO_2	Al_2O_3	FeOT	MnO	MgO	CaO	Na_2O	K_2O	P_2O_5	Cl	count
VG-2	1.3	9.8	2.5	4.8	22.2	3.2	3.4	7.2	28.4	25.1	105.1	204
VG-2_UAF	1.8	4.1	2.2	3.3	21.3	3.9	1.9	7.4	19.6	36.9	52.9	34
VG-2_CalVO	0.9	10.3	1.5	1.9	20.7	2.0	3.6	4.0	26.6	18.6	35.4	155
A-99	1.3	5.1	3.3	5.1	27.1	4.4	2.7	8.2	13.3	13.7	170.9	108
A-99_UAF	1.5	3.2	2.8	4.5	23.2	3.8	3.1	10.3	12.9	17.0	61.0	82
BG-3	2.1	6.0	3.6	6.0	30.4	10.8	6.8	22.1	59.3	44.7	254.2	104
VG-568	0.6	75.9	1.9	13.5	198.4	90.8	12.1	8.5	6.4	1,208.1	40.8	92
VG-568_UAF	1.0	48.7	2.5	9.3	149.9	49.2	9.9	23.2	5.6	579.6	21.9	127
RLS-132	0.6	32.8	2.5	8.0	29.1	43.0	36.6	5.0	6.7	Inf	21.4	89
RLS-75	0.7	91.7	1.1	8.1	110.9	Inf	19.5	4.3	5.9	2,285.5	10.9	24
KN-18	0.9	38.8	3.5	6.8	79.1	Inf	229.3	6.2	6.6	638.4	15.1	99
CCNM	1.1	58.9	2.1	6.3	52.0	39.6	6.2	22.6	5.6	460.2	8.2	21

Accuracy is assessed as the measured concentration divided by the accepted literature concentration for each standard (multiplied by 100 to express as a percentage). Results are shown in table 2. With few exceptions, the accuracy of average glass measurements is within 2σ reproducibility of the accepted literature value (fig. 4).

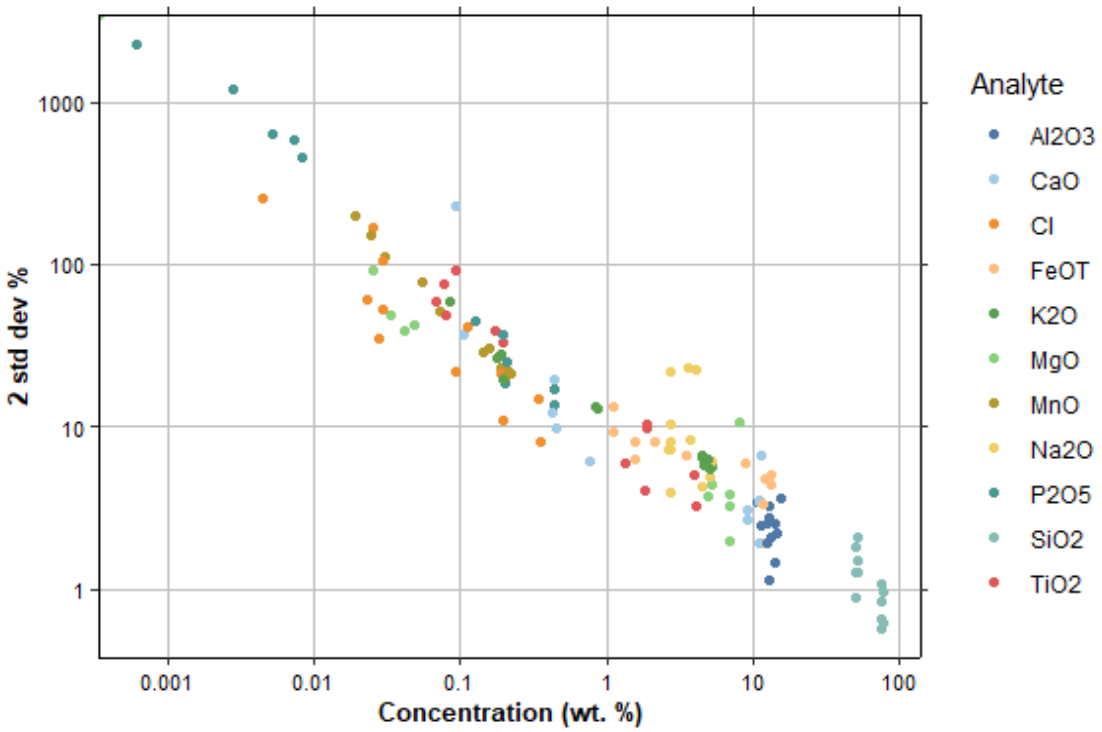

Figure 2. Log-linear relationship between concentration and precision for different analytes in repeat analyses of secondary standards.

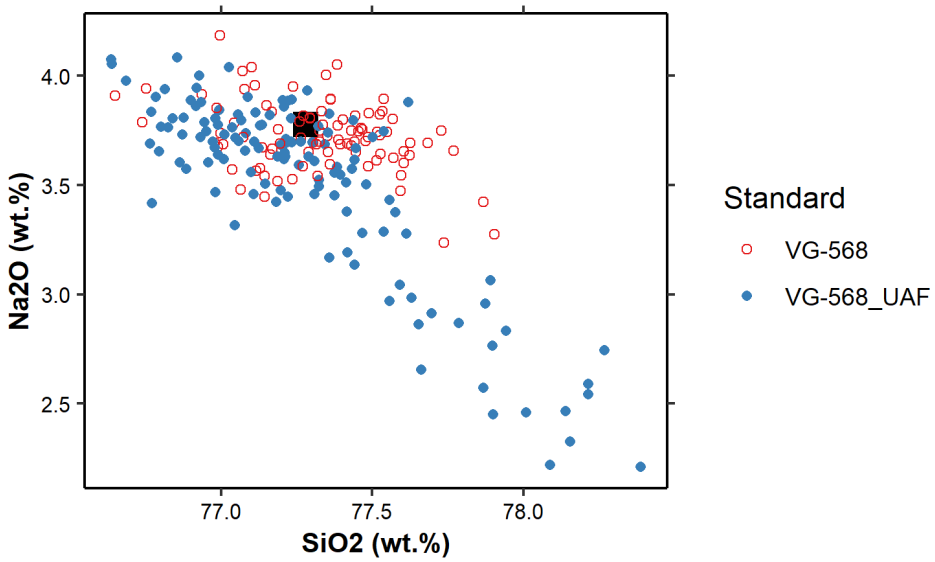

Figure 3. Results for UAF standard block VG-568 glass to removable standard block glass VG-568. Literature-accepted values are shown as a black square. Na loss is evident only on glass chips that are part of the internal standard block.

Table 2. Accuracy of repeat secondary standard analysis reported as 100 * measured/accepted concentrations.

Standard	SiO_2	TiO_2	Al_2O_3	FeOT	MnO	MgO	CaO	Na_2O	K_2O	P_2O_5	Cl	count
VG-2	99.7	100.6	100.5	100.8	96.8	100.9	99.3	103.7	99.2	103.3		204
VG-2_UAF	100.2	99.7	102.2	97.8	99.8	99.3	99.1	100.2	102.2	97.4		34
VG-2_CalVO	99.9	100.5	100.4	101.0	94.9	100.7	98.2	103.8	93.7	102.0		155
A-99	99.9	97.8	101.0	99.2	124.3	100.8	98.6	101.5	100.6	114.7		108
A-99_UAF	100.2	98.5	102.1	97.9	125.7	97.5	97.9	101.4	106.1	116.0		82
BG-3	99.7	101.4	101.2	98.3	93.8	97.0	99.8	109.3		106.9		104
VG-568	100.1	64.4	101.2	88.7			85.6	98.4	99.2			92
VG-568_UAF	99.9	65.5	102.2	89.1			90.0	96.9	102.0			127
RLS-132	100.6	92.9	100.3	100.3	95.4	95.9	87.7	97.4	98.3	0.0	102.1	89
RLS-75	100.9	103.2	102.3	99.1	76.8		91.5	103.0	98.9		98.0	24
KN-18	100.1	93.4	100.8	99.9	90.6		62.8	92.0	99.9			99
CCNM	99.4		100.7	99.9			101.7	99.0	103.2		104.4	21

Exceptions to this (Cl in VG-2, Mn in A-99_UAF, Ca in VG-568, Fe in VG-568_UAF, and Ca and Na in KN-18) are in minor or trace elements where uncertainties are generally high in measured and literature determinations. SiO_2, the largest oxide constituent of any volcanic glass, has relative accuracy ± 0.5 percent for all basalt to rhyolite compositions. There is no systematic under or over-estimation for low or high Si concentrations.

Concentrations of Al_2O_3, however, are consistently 1–2 percent higher relative to literature values (except RLS-132). While within the 2σ reproducibility, this systematic offset suggests some slight error in our calibration, background correction, or offset in the literature values. Concentrations of FeOT are also consistently 1–2 percent lower than literature values in low SiO_2 glasses, despite concentrations being higher with subsequently lower uncertainty. Like Al_2O_3, while these values are within 2σ reproducibility, the systematic offset is notable and could result in bias in comparison to other datasets using different calibration strategies. There was no observed difference in FeOT calibrations using ilmenite (May and October 2018) vs. fayalite (all other sessions).

Variations between analytical sessions are shown in a series of "Harker" style discrimination diagrams, where each major element oxide is plotted against SiO_2 in a separate panel for each standard. Points are colored by session date. These plots are provided in the appendix (app. A). Chlorine, a minor to trace element in volcanic glass, has concentrations showing apparent session-to-session offsets, with lower concentration results for 2020–2022

sessions and higher in 2018 and 2019 (fig. 5). Despite this apparent difference in secondary standards, two samples of matrix glass from Redoubt Volcano (AT-1389, AT-1405) were analyzed for Cl in both May 2019 and January 2022 (results of these repeat glass analyses are provided in the **RepeatUnkns** table), resulting in median Cl concentrations that are identical at 0.18 wt.% (fig. 5). This suggests that corrections between methods on these dates might not be warranted.

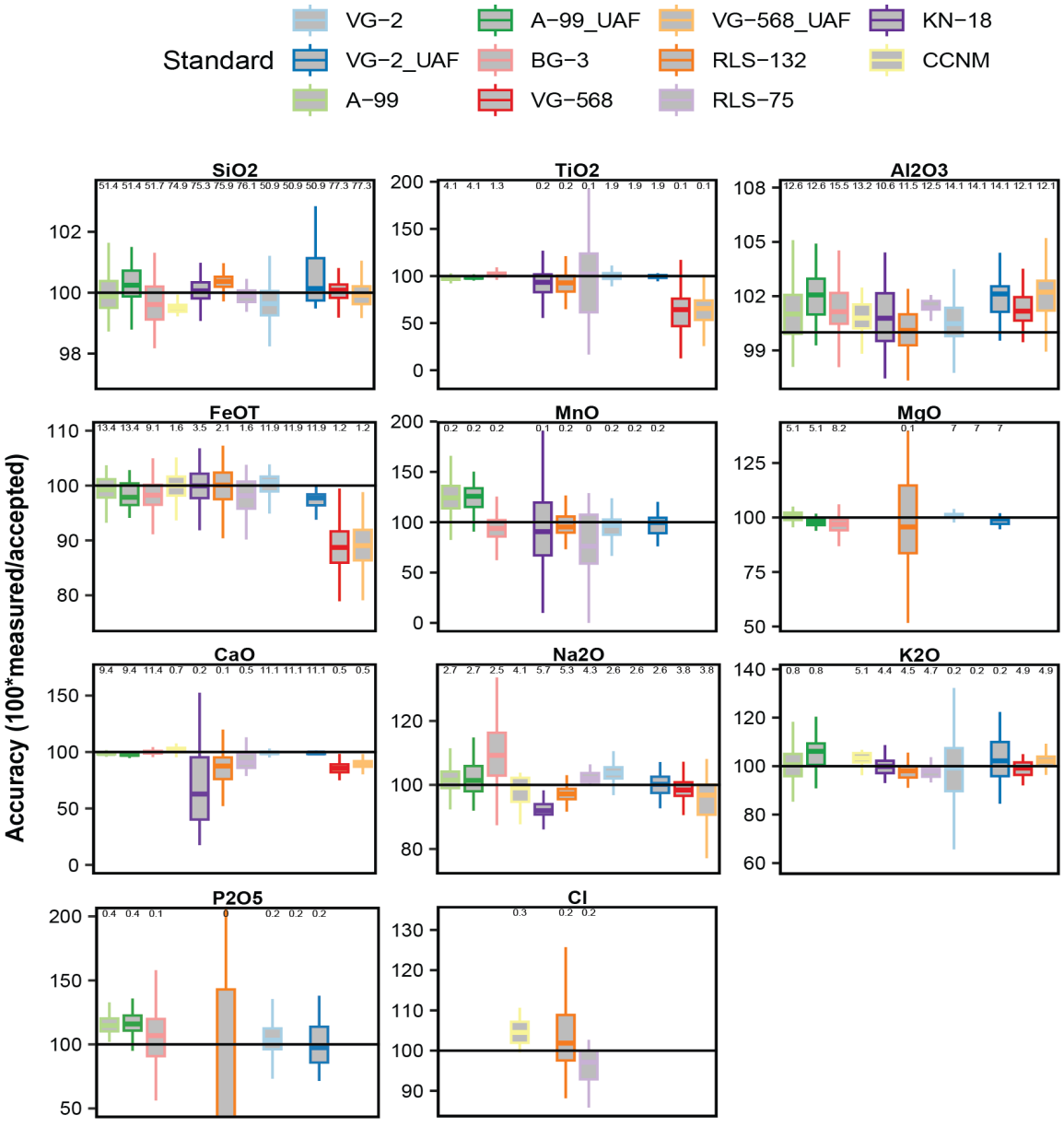

Figure 4. Accuracy (100*measured/accepted) plots for all major oxides. Standard concentrations (in wt.%) are annotated above box plots. Box plot horizontal lines show the lower quartile, median, and upper quartile, while lines extend to the minimum and maximum values within 1.5x the interquartile

range, excluding outliers. P_2O_5 plot clips range of RLS-132 due to high uncertainty at very low concentrations.

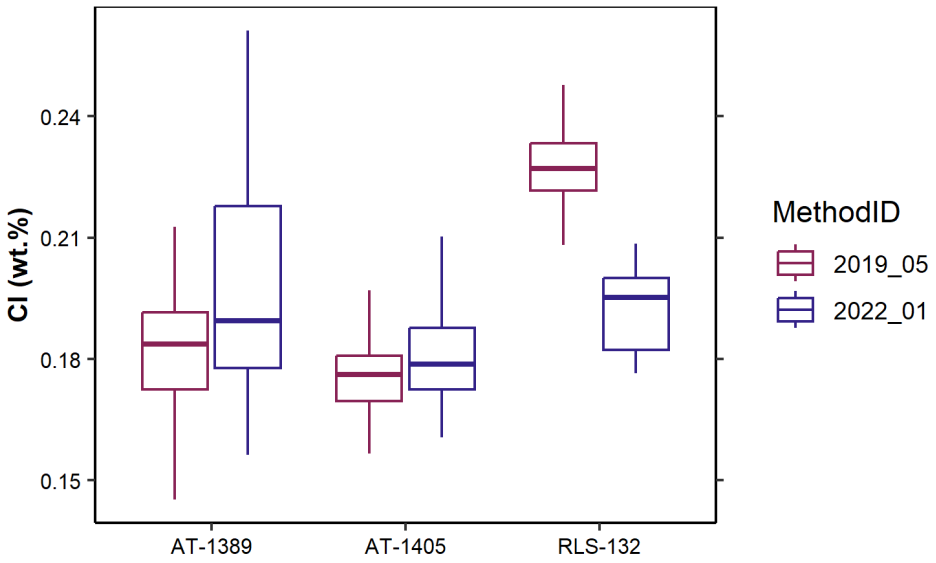

Figure 5. Cl concentration results (wt.%) for repeat analyses of two Redoubt tephra samples on sessions with apparent differences in Cl values for secondary standards (RLS-132 shown). The similarity of Cl in these two samples suggests that the secondary standards may have some Cl heterogeneity. See figure 4 for a boxplot explanation.

DISCUSSION

Results of secondary standard analyses demonstrate good reproducibility and accuracy for glasses following our reported EPMA method. Importantly, by aggregating uncertainty results over multiple analytical sessions and years, we demonstrate long-term comparability of results important for tephra correlation and petrologic studies (Lowe and others, 2017).

These results provide the foundation to explore and test future improvements to our analytical routine. The strong correlation between concentration and reproducibility suggests a demonstrated effective limit of quantification for our analyses. Trace concentrations below 0.01 wt.% all have >100 percent uncertainty. This threshold is reached between 0.01 and 0.1 wt.% for all elements, suggesting extreme caution should be applied when interpreting values for trace element analyses. Longer peak count times should allow for better analysis at low concentrations; however, within our typical peak times of 10 to 30 seconds, we do not see particularly strong improvements in precision (fig. 6). Both the UAF and USGS Menlo Park laboratories are considering adding simultaneous energy-dispersive x-ray spectroscopy (EDS) capabilities, which may allow longer analysis of minor elements by analyzing high-concentration components (e.g., SiO_2, Al_2O_3) on the EDS detector.

Failure to enable the TDI correction during the two sessions on the USGS Menlo Park EPMA did not appear to result in significant Na loss in our secondary standards. However, some caution is warranted in interpreting unknown glasses from these sessions, especially

those that may be hydrated and thus more sensitive to Na migration. Future analyses on all instruments will include this correction.

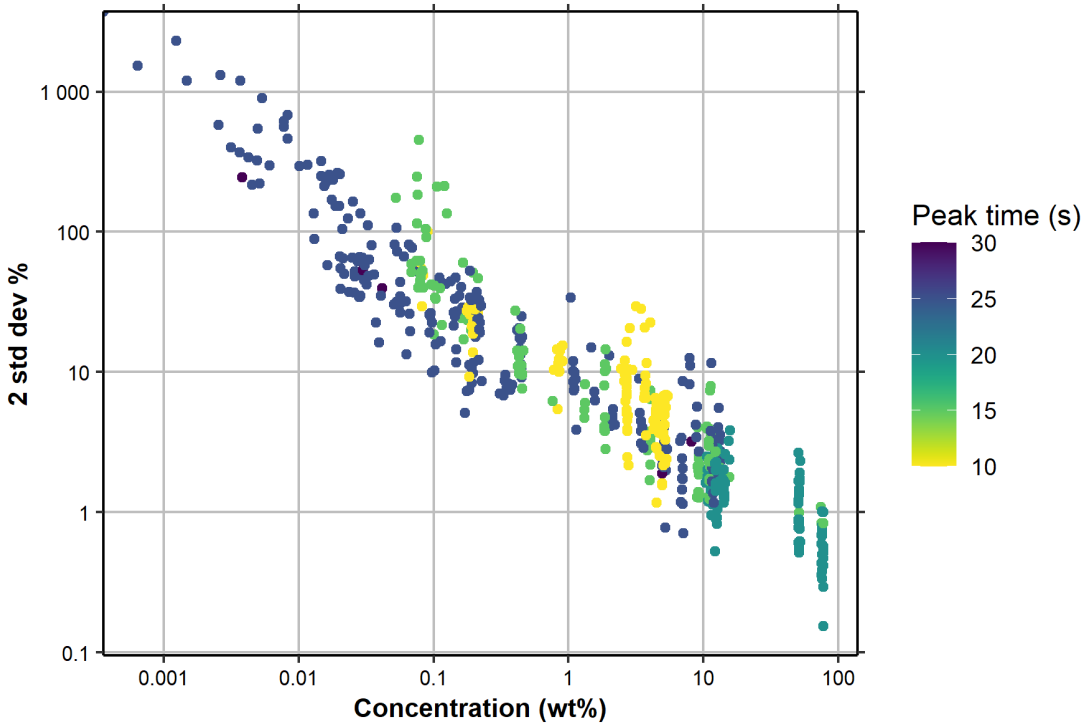

Figure 6. Consideration of individual analyte peak counting time with uncertainty of secondary standards (compare to figure 2).

Future secondary standard results will be reported in subsequent versions. By maintaining a long-term record of secondary standard results, we hope to identify any systematic changes through time and correct these to provide comparable results between studies. Future improvements or identification of the need to adjust unknown data reported here can be discussed and justified in future iterations. All matrix glass analyses from Alaska tephra will be stored in the Geological Database of Information on Volcanoes in Alaska (GeoDIVA; Cameron and others, 2019; Cameron and others, 2022). If a need for systematic changes in previously reported analyses is found and justified in this data series, these adjustments can be made to the analyses in the database, like adjustments made to trace element bulk chemical data (Nye and others, 2018).

ACKNOWLEDGEMENTS

This article has been peer-reviewed and approved for publication consistent with USGS Fundamental Science Practices (pubs.usgs.gov/circ/1367). We appreciate reviews provided by Heather Lowers and Steve Kuehn, metadata review by Simone Montayne, and editorial handling by Kristen Janssen. Any use of trade, firm, or product names is for descriptive purposes only and does not imply endorsement by the U.S. Government.

REFERENCES

Armstrong, J.T., 1988, Quantitative analysis of silicates and oxide minerals: Comparison of Monte-Carlo, ZAF and Phi-Rho-Z procedures: Microbeam Analysis, p. 239–246

Cameron, C.E., Crass, S.W., and AVO Staff, eds., 2022, Geologic Database of Information on Volcanoes in Alaska (GeoDIVA): Alaska Division of Geological & Geophysical Surveys Digital Data Series 20. https://doi.org/10.14509/30901

Cameron, C.E., Mulliken, K.M., Crass, S.W., Schaefer, J.R., and Wallace, K.L., 2019, Alaska Volcano Observatory geochemical database, version 2: Alaska Division of Geological & Geophysical Surveys Digital Data Series 8 v. 2, 22 p. https://doi.org/10.14509/30058

Helz, R.T., Clague, D.A., Mastin, L.G., and Rose, T.R., 2014, Electron microprobe analyses of glasses from Kīlauea Tephra Units, Kīlauea Volcano, Hawaii: U.S. Geological Survey Open-File Report 2014–1090, 24 p., plus 2 appendixes in separate files. https://dx.doi.org/10.3133/ofr20141090

Jarosewich, E., Nalen, J.A., and Norberg, J.A., 1980, Reference Samples for Electron Microprobe Analysis: Geostandards Newsletter 4, p. 43–47. https://doi.org/10.1111/j.1751-908X.1980.tb00273.x

Kuehn, S.C., Froese, D.G., Shane, P.A., and INTAV Intercomparison Participants, 2011, The INTAV intercomparison of electron-beam microanalysis of glass by tephrochronology laboratories: results and recommendations: Quaternary International v. 246, no. 1–2, p.19–47.

Lowe, D.J., Pearce, N.J.G., Jorgensen, M.A., Kuehn, S.C., Tryon, C.A., and Hayward, C.L., 2017, Correlating tephras and cryptotephras using glass compositional analyses and numerical and statistical methods: Review and evaluation: Quaternary Science Reviews 175, p. 1–44. http://dx.doi.org/10.1016/j.quascirev.2017.08.003

Macdonald, R., Smith, R.L., and Thomas, J.E., 1992, Chemistry of the subalkalic silicic obsidians: U.S. Geological Survey Professional Paper 1523, 214 p. https://pubs.usgs.gov/pp/1523

Nielsen, C.H., and Sigurdsson, H., 1981, Quantitative methods for electron micro-probe analysis of sodium in natural and synthetic glasses: American Mineralogist, v. 66, p. 547–552.

Nye, C.J., Begét, J.E., Layer, P.W., Mangan, M.T., McConnell, V.S., McGimsey, R.G., Miller, T.P., Moore, R.B., and Stelling, P.L., 2018, Geochemistry of some Quaternary lavas from the Aleutian Arc and Mt. Wrangell: Alaska Division of Geological and Geophysical Surveys Raw Data File 2018-1, 29 p. https://doi.org/10.14509/29843

Probe for EPMA [Computer software], 2023, Probe Software, Inc. https://probesoftware.com/Update.html

Wallace, K.L., Bursik, M.I., Kuehn, Stephen, Kurbatov, A.V., Abbott, Peter, Bonadonna, Costanza, Cashman, Katharine, Davies, S.M., Jensen, Britta, Lane, Christine, Plunkett, Gill, Smith, V.C., Tomlinson, Emma, Thordarsson, Thor, and Walker, J.D., 2022, Community established best practice recommendations for tephra studies—from collection through analysis: Scientific Data, v. 9, p. 447. https://doi.org/10.1038/s41597-022-01515-y

APPENDIX A: HARKER STYLE DISCRIMINATION DIAGRAMS

Al_2O_3

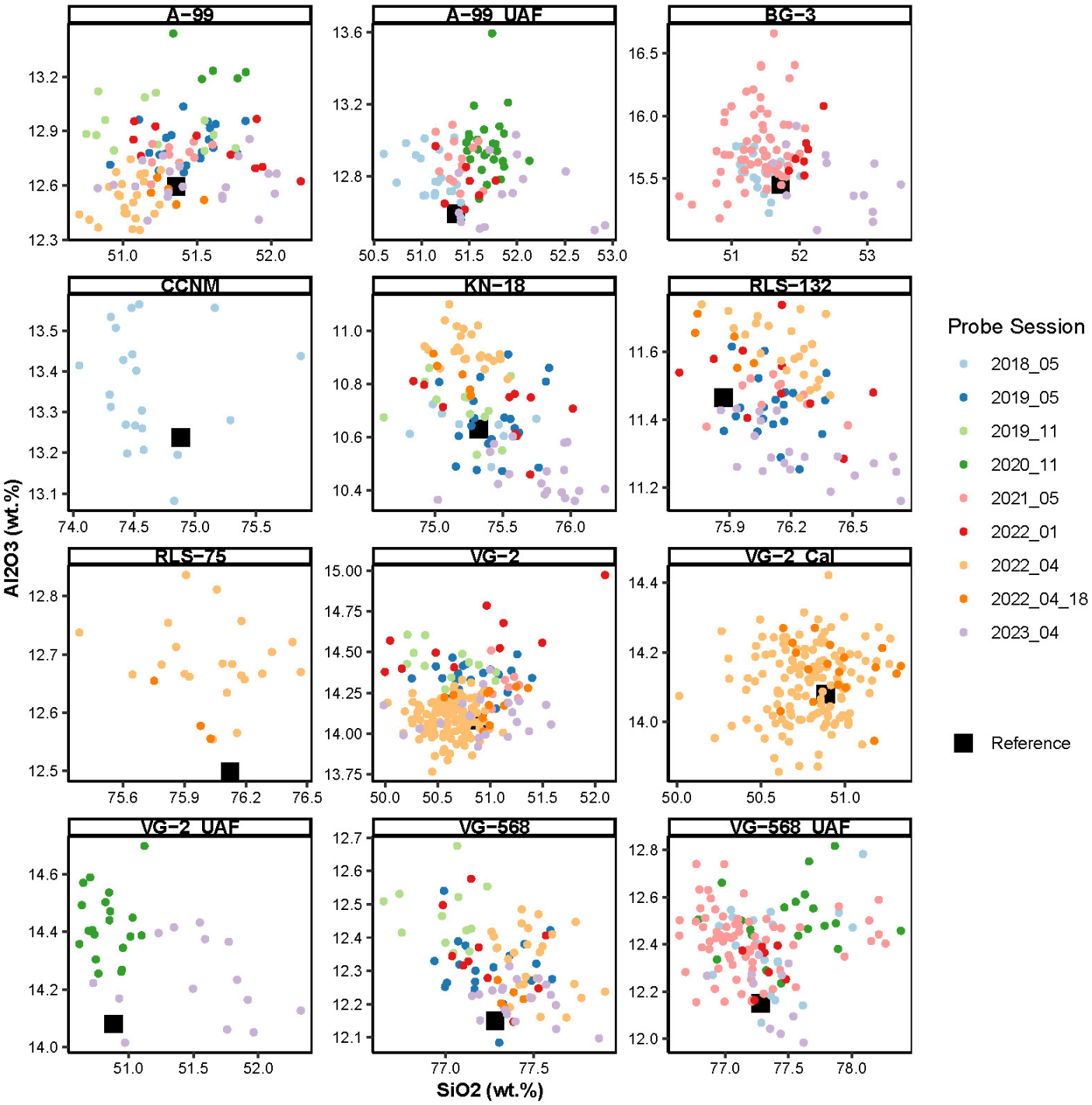

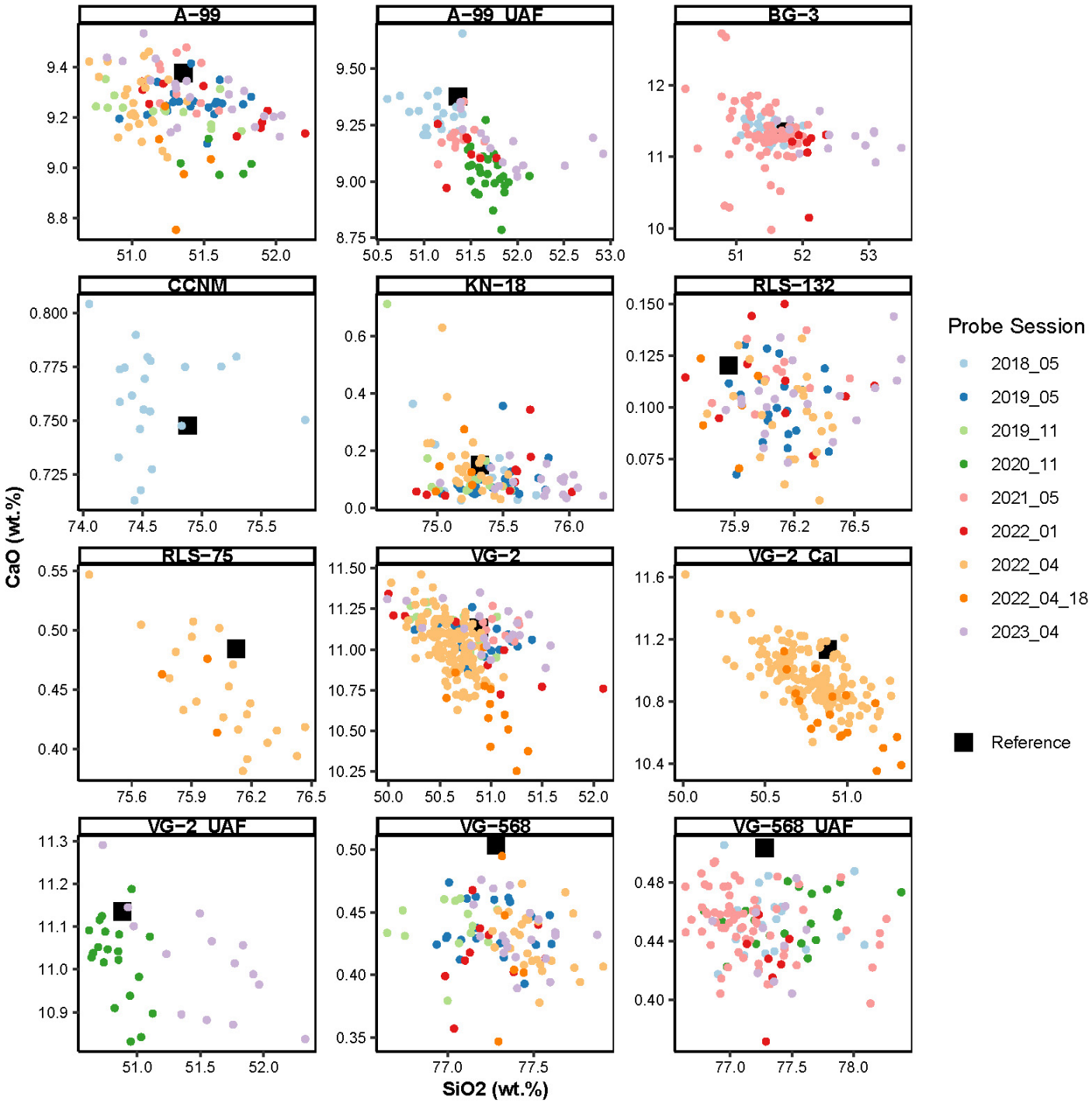
CaO
A-99
A-99_UAF
BG-3
CCNM
KN-18
RLS-132
RLS-75
VG-2
VG-2_Cal
VG-2_UAF
VG-568
VG-568_UAF
CaO (wt.%)
SiO2 (wt.%)
Probe Session
2018_05
2019_05
2019_11
2020_11
2021_05
2022_01
2022_04
2022_04_18
2023_04
Reference

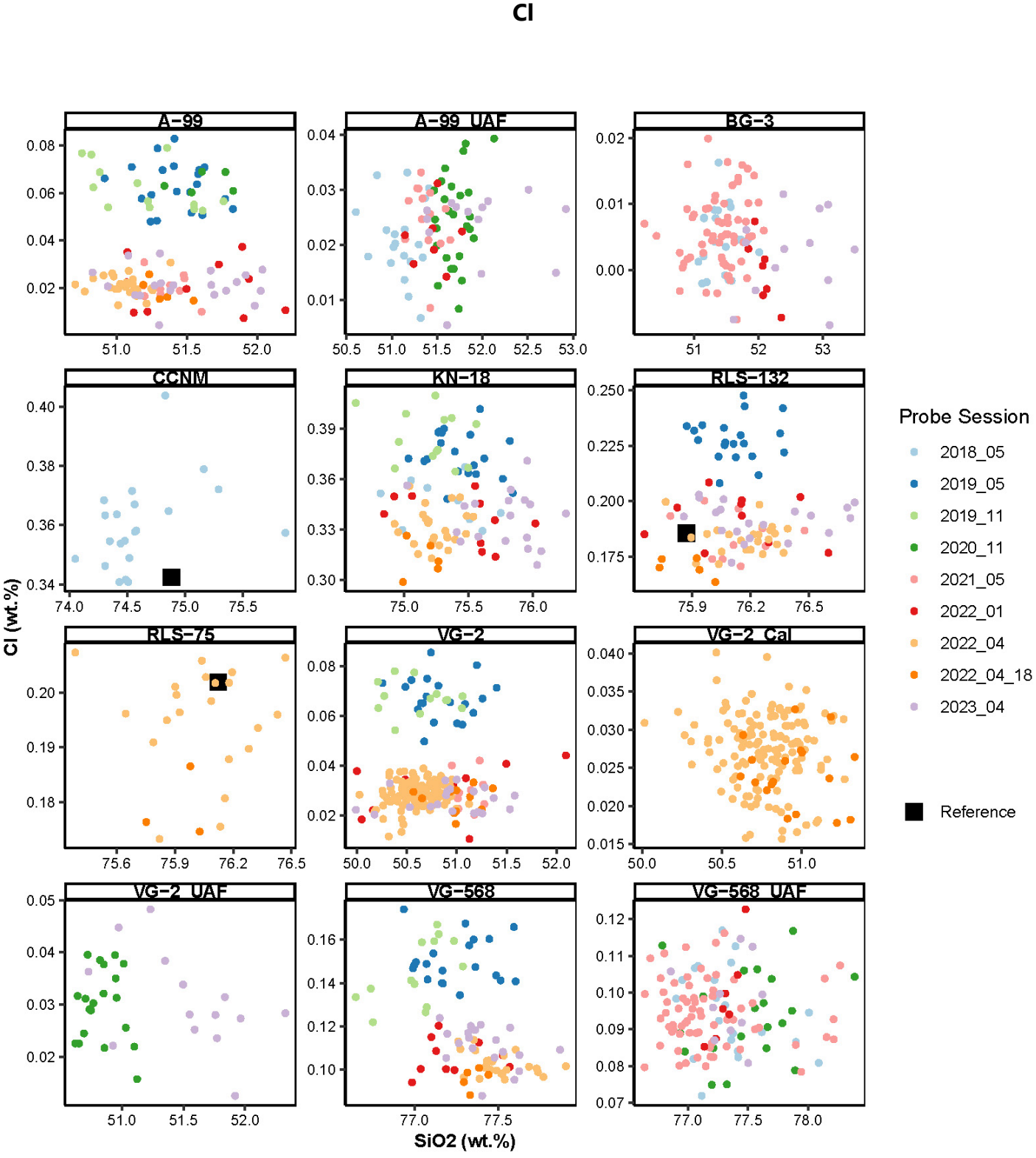
Cl
A-99
A-99_UAF
BG-3
CCNM
KN-18
RLS-132
RLS-75
VG-2
VG-2_Cal
VG-2_UAF
VG-568
VG-568_UAF
Cl (wt.%)
SiO2 (wt.%)
Probe Session
2018_05
2019_05
2019_11
2020_11
2021_05
2022_01
2022_04
2022_04_18
2023_04
Reference

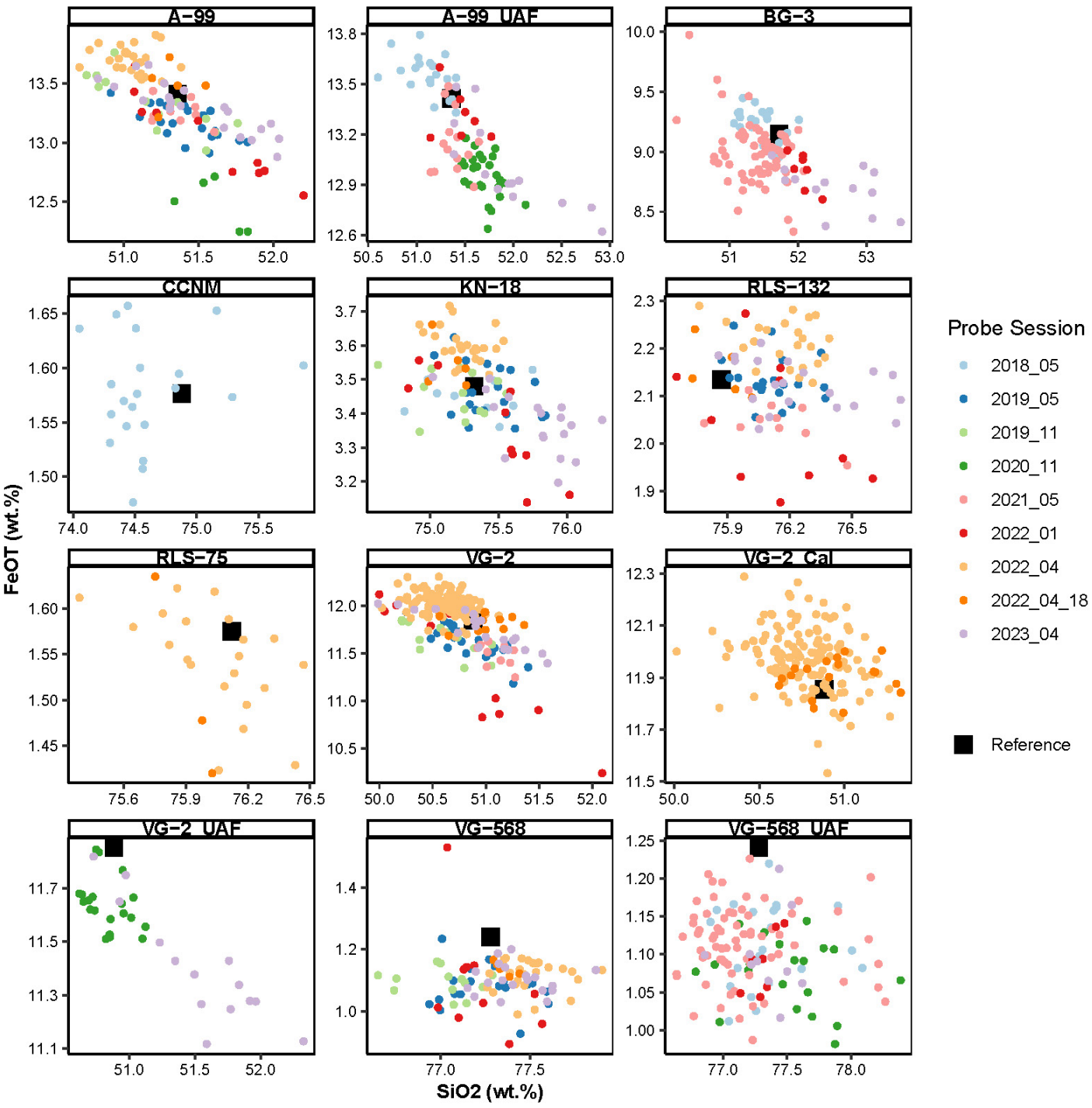
FeOT
A-99
A-99_UAF
BG-3
CCNM
KN-18
RLS-132
RLS-75
VG-2
VG-2_Cal
VG-2_UAF
VG-568
VG-568_UAF
FeOT (wt.%)
SiO2 (wt.%)
Probe Session
2018_05
2019_05
2019_11
2020_11
2021_05
2022_01
2022_04
2022_04_18
2023_04
Reference

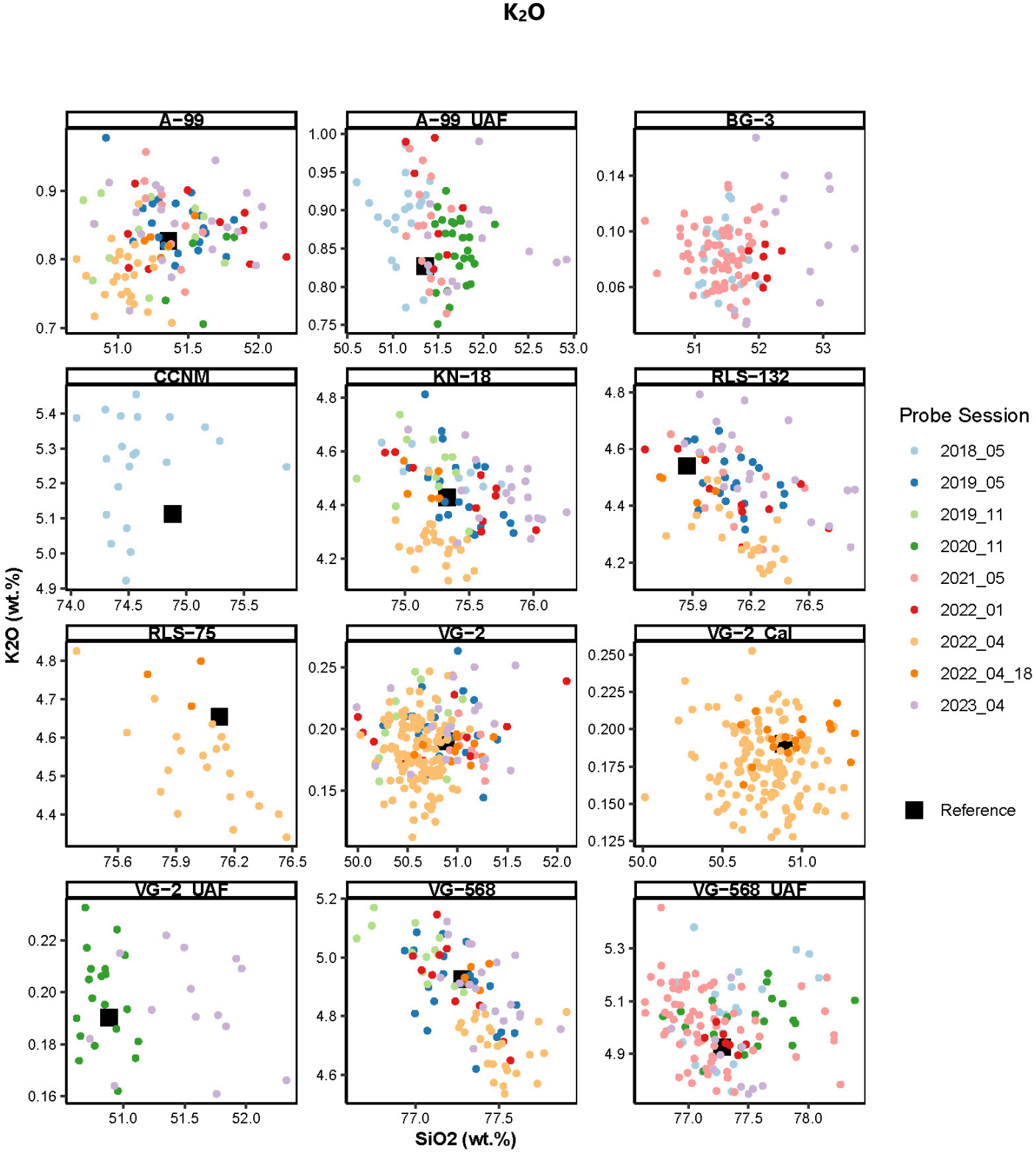
K2O
A-99
A-99_UAF
BG-3
CCNM
KN-18
RLS-132
RLS-75
VG-2
VG-2_Cal
VG-2_UAF
VG-568
VG-568_UAF
K2O (wt.%)
SiO2 (wt.%)
Probe Session
2018_05
2019_05
2019_11
2020_11
2021_05
2022_01
2022_04
2022_04_18
2023_04
Reference

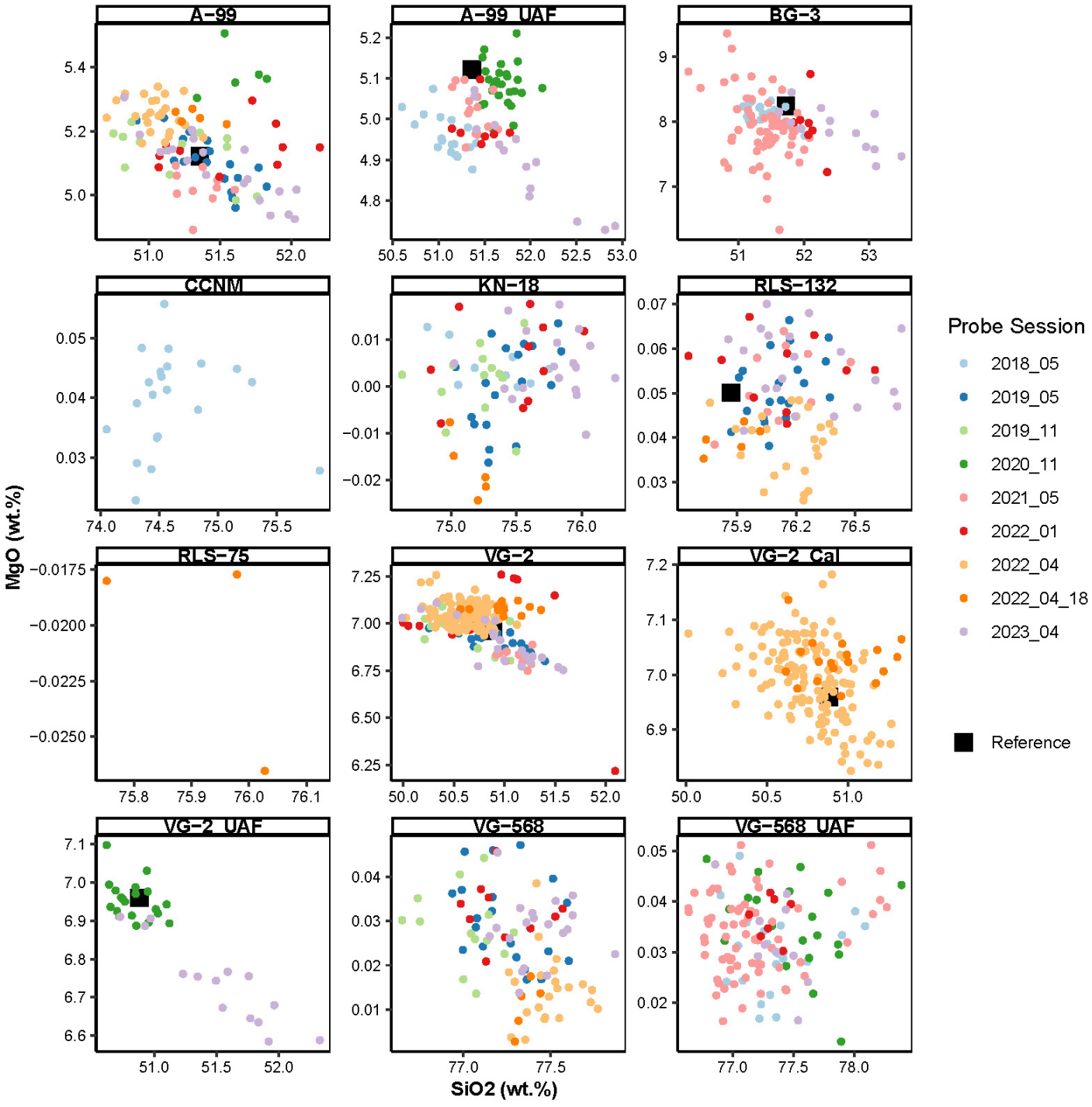
MgO
A-99
A-99_UAF
BG-3
CCNM
KN-18
RLS-132
RLS-75
VG-2
VG-2_Cal
VG-2_UAF
VG-568
VG-568_UAF
MgO (wt.%)
SiO2 (wt.%)
Probe Session
2018_05
2019_05
2019_11
2020_11
2021_05
2022_01
2022_04
2022_04_18
2023_04
Reference

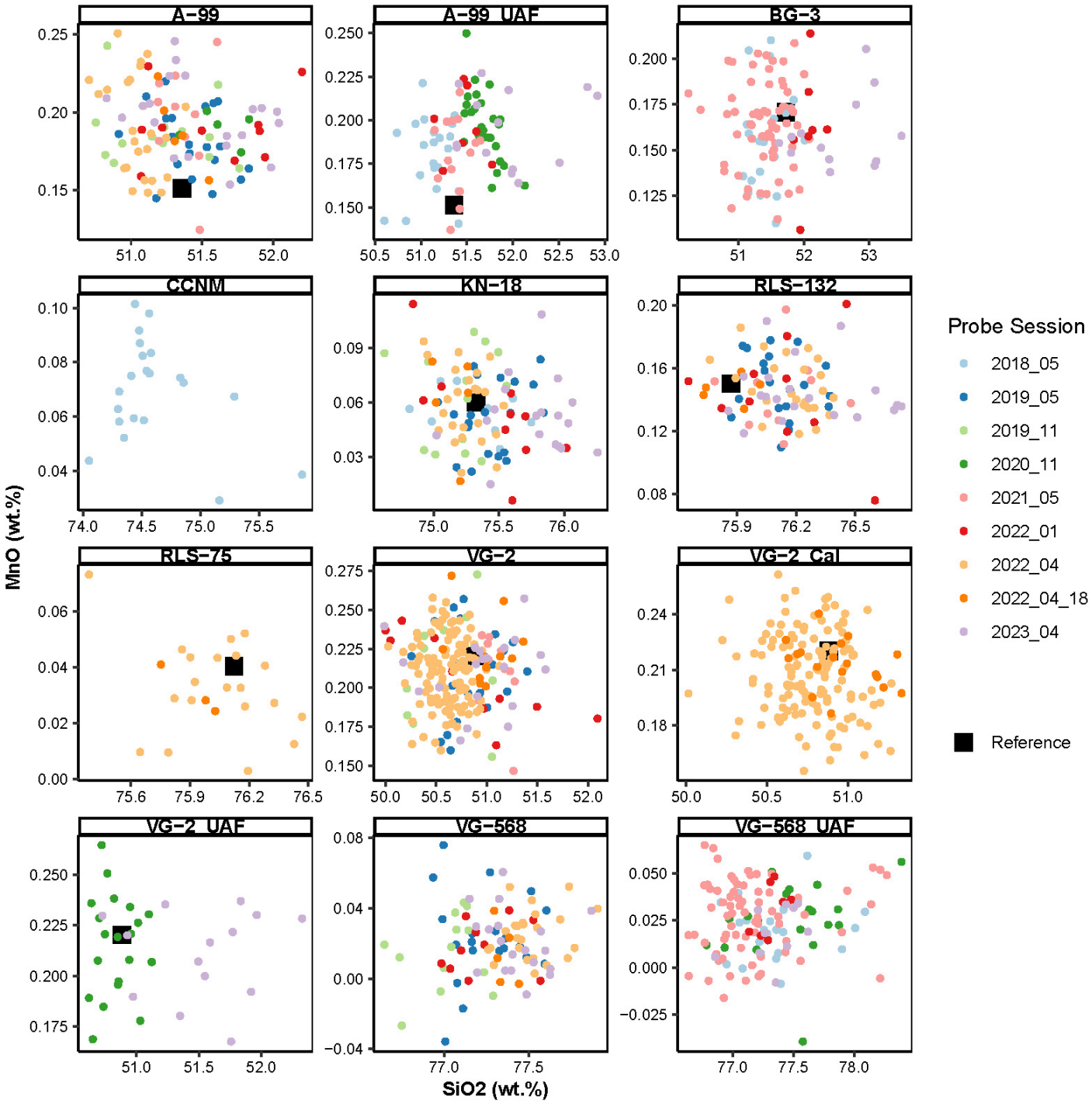
MnO
A-99
A-99_UAF
BG-3
CCNM
KN-18
RLS-132
RLS-75
VG-2
VG-2_Cal
VG-2_UAF
VG-568
VG-568_UAF
MnO (wt.%)
SiO2 (wt.%)
Probe Session
2018_05
2019_05
2019_11
2020_11
2021_05
2022_01
2022_04
2022_04_18
2023_04
Reference

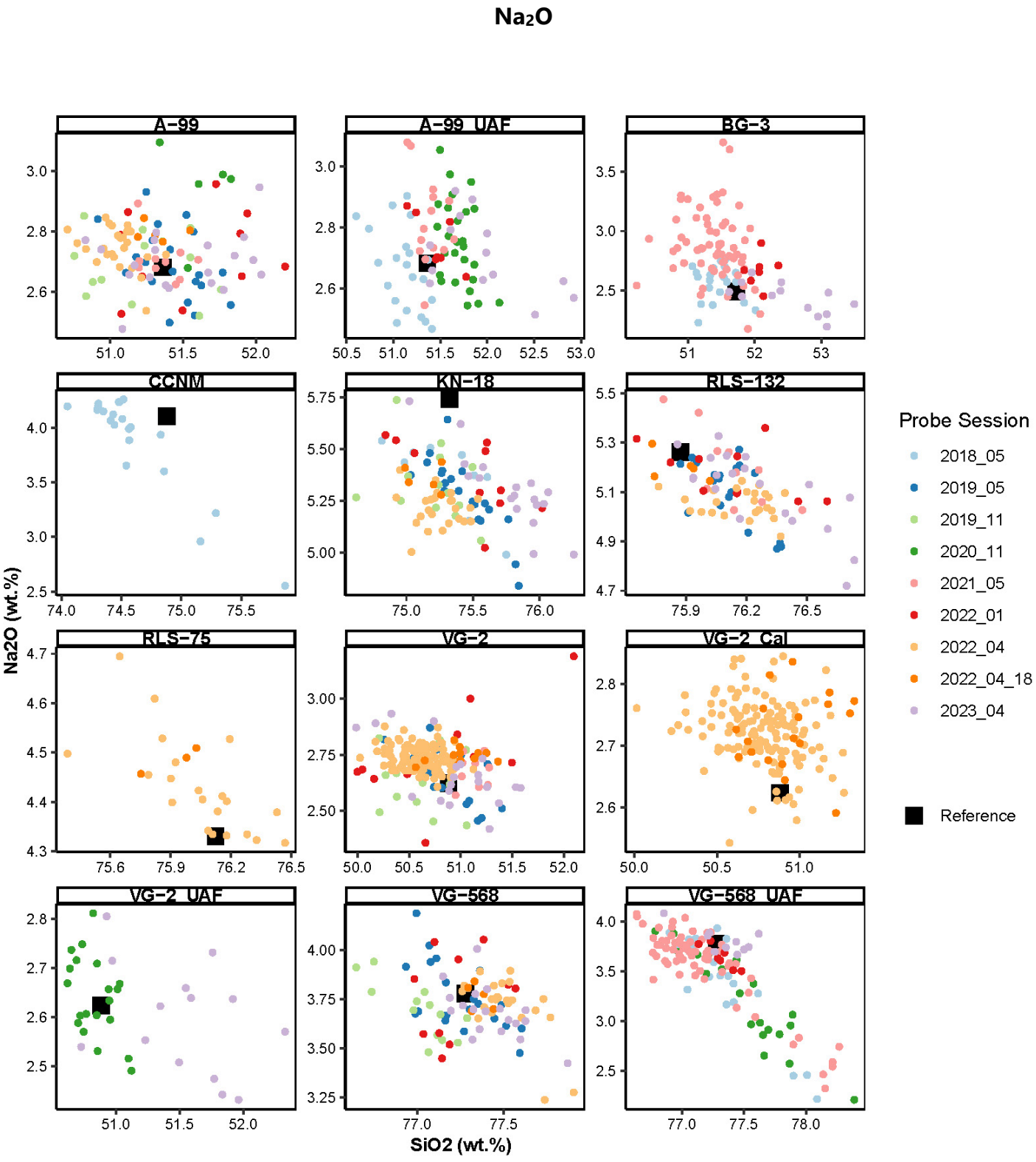
Na2O
A-99
A-99_UAF
BG-3
CCNM
KN-18
RLS-132
RLS-75
VG-2
VG-2_Cal
VG-2_UAF
VG-568
VG-568_UAF
Na2O (wt.%)
SiO2 (wt.%)
Probe Session
2018_05
2019_05
2019_11
2020_11
2021_05
2022_01
2022_04
2022_04_18
2023_04
Reference

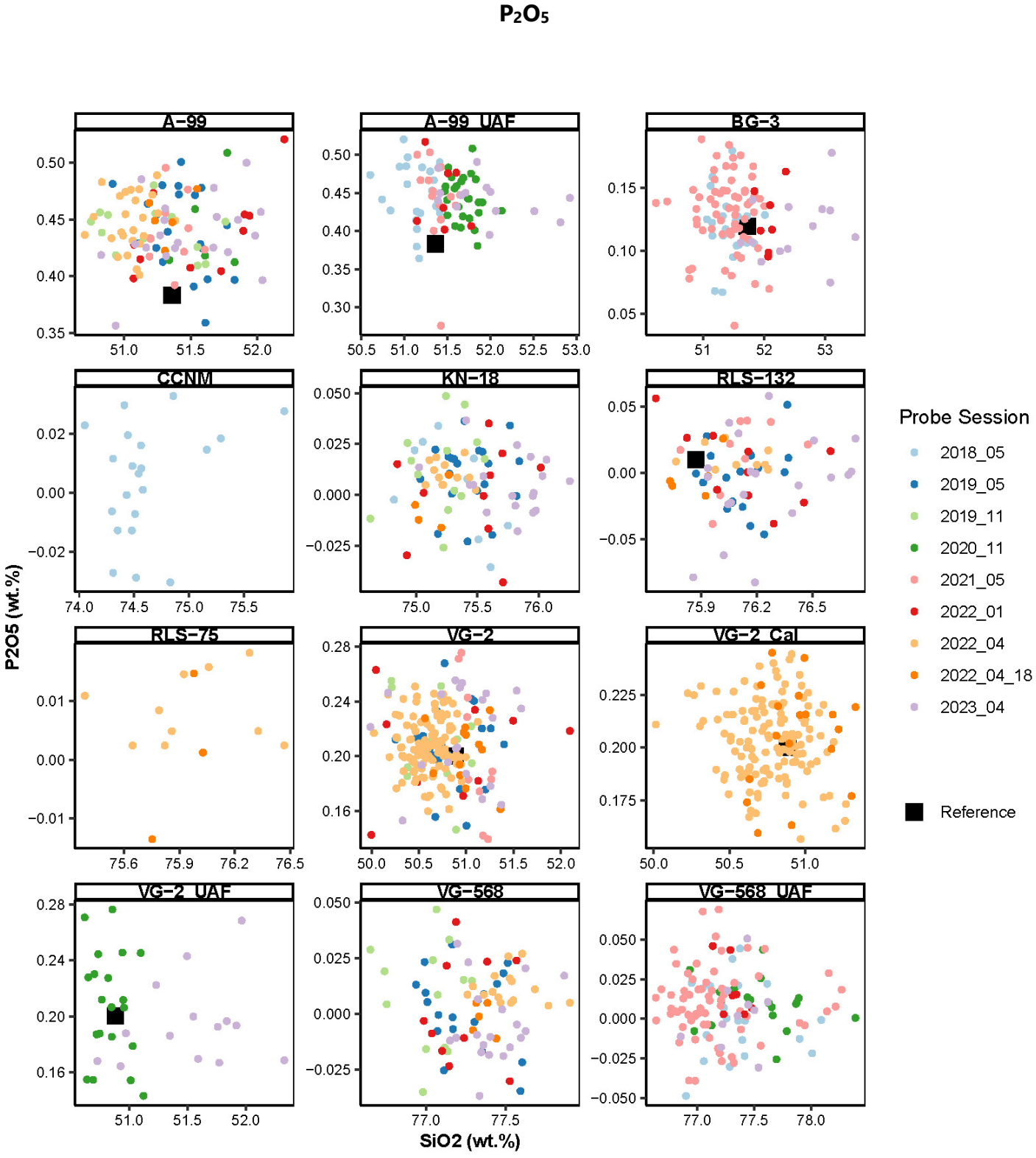
P2O5
A-99
A-99_UAF
BG-3
CCNM
KN-18
RLS-132
RLS-75
VG-2
VG-2_Cal
VG-2_UAF
VG-568
VG-568_UAF
P2O5 (wt.%)
SiO2 (wt.%)
Probe Session
2018_05
2019_05
2019_11
2020_11
2021_05
2022_01
2022_04
2022_04_18
2023_04
Reference

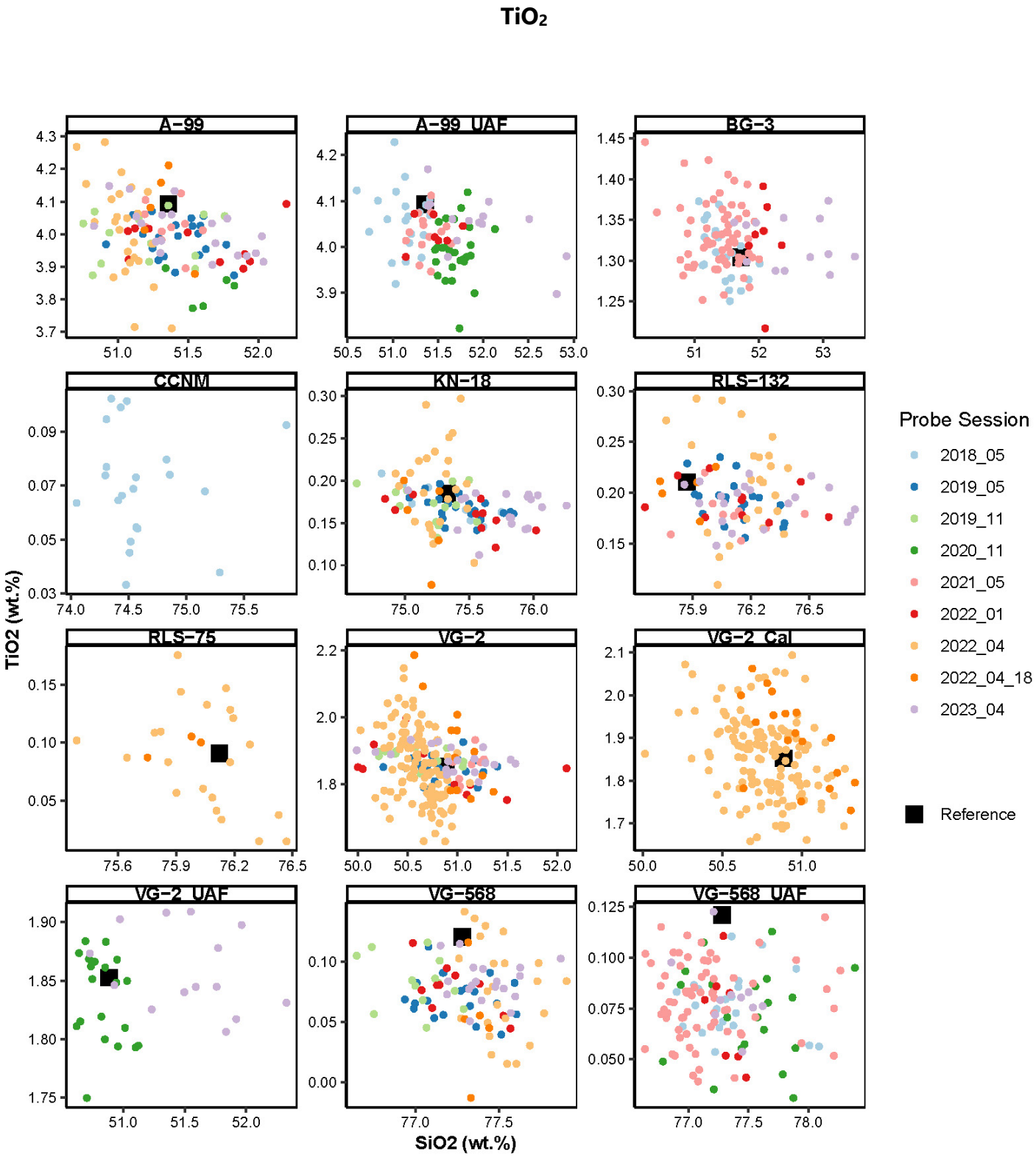
TiO2
A-99
A-99_UAF
BG-3
CCNM
KN-18
RLS-132
RLS-75
VG-2
VG-2_Cal
VG-2_UAF
VG-568
VG-568_UAF
TiO2 (wt.%)
SiO2 (wt.%)
Probe Session
2018_05
2019_05
2019_11
2020_11
2021_05
2022_01
2022_04
2022_04_18
2023_04
Reference